

**Sulfuric Acid Monohydrate:  
Formation and Heterogeneous Chemistry in the Stratosphere**

Renyi Zhang, Ming-Tsun Leu, and Leon F. Keyser  
Earth and Space Sciences Division  
Jet Propulsion Laboratory  
California Institute of Technology  
Pasadena, CA 91109

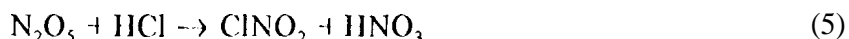
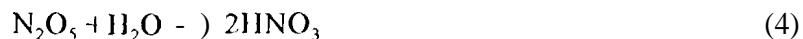
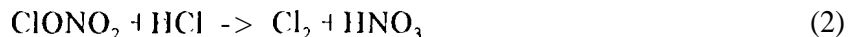
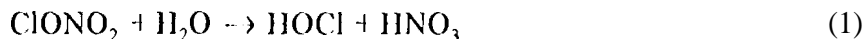
(Submitted to *JGR*, Oct. 20, 1994)

## Abstract

We have investigated some thermodynamic properties (i.e. freezing/melting points) and heterogeneous chemistry of sulfuric acid monohydrate (SAM,  $\text{H}_2\text{SO}_4 \cdot \text{H}_2\text{O}$ ), using a fast flow-reactor coupled to a quadrupole mass spectrometer. The freezing point observations show that for sulfuric acid contents between 75 and 85 wt% the monohydrate crystallizes readily at temperatures between 220 and 240 K. Once formed, SAM can be thermodynamically stable in the  $\text{H}_2\text{O}$  partial pressure range of  $(1-4) \times 10^{-4}$  Torr and in the temperature range of 220-240 K. For a given  $\text{H}_2\text{O}$  partial pressure, SAM melts at lower temperatures. The reaction probability measurements indicate that the hydrolysis of  $\text{N}_2\text{O}_5$  is significantly suppressed due to the formation of crystalline SAM: the reaction probability on water-rich SAM is on the order of  $10^{-3}$  at 210 K and decreases by more than an order of magnitude for the acid-rich form. The hydrolysis rate of  $\text{ClONO}_2$  on water-rich SAM is even smaller, on the order of  $10^{-4}$  at 195 K. No enhancement of these reactions is observed in the presence of 1 ICl vapor at the stratospheric concentrations, in addition, BET analysis of gas-adsorption isotherms has been performed to characterize the surface roughness and porosities of the SAM substrates. The results suggest the possible formation of SAM in some regions of mid- or low latitude stratosphere and, consequently, much slower heterogeneous reactions on these frozen aerosols.

## Introduction

It is now well recognized that the high rates of Antarctic ozone destruction are induced by surface-catalyzed reactions on polar stratospheric cloud (PSC) particles [Solomon, 1988]. The heterogeneous reactions of primary interest in the stratosphere are as follows,



These reactions transform stable chlorine reservoir compounds into photochemically active forms which are rapidly converted into the chlorine radicals (Cl and ClO), leading to catalytic ozone destruction. Of equal importance to the polar stratospheric ozone depletion is the concomitant repartitioning of nitrogen species ( $\text{NO}_x$ ) from the gas phase to the condensed phase (in the form of  $\text{NO}_y$ ) since they can be removed irreversibly from the stratosphere due to gravitational sedimentation of PSC particles. If significant  $\text{HNO}_3$  remains in the polar spring, the chlorine radicals will be converted back to  $\text{ClONO}_2$  by the reaction of ClO and  $\text{NO}_2$  produced from  $\text{HNO}_3$  photolysis, halting ozone depletion,

The PSC particles which act as catalysts for the heterogeneous reactions are generally classified as nitric acid trihydrates (type I) and water-ice (type II) [Crutzen and Arnold, 1986; Toon et al., 1986]. Laboratory studies have demonstrated that the heterogeneous reactions proceed readily on the proposed PSC materials [DeMore et al., 1992; Kolb et al., 1994]. Also, the occurrence of heterogeneous reactions on particles in the polar regions during winter and early spring has been clearly seen in field observations, showing chemical changes such as the increase in ClO and concurrent decreases in Cl,  $\text{ClONO}_2$ , and ozone as measured from inside to outside of the chemically perturbed regions in Antarctica and the Arctic [Anderson et al., 1991; Brune et al., 1991; Webster et al., 1993].

Sulfate aerosols in the stratosphere have also been proposed to affect the balance of global ozone via heterogeneous reactions analogous to those implicated in polar ozone loss [Hofmann and Solomon, 1988; Brasseur et al., 1991; Rodriguez et al., 1991]. The sulfate aerosol layer,

which exists at latitudes between 10 and 30 km, is composed of sulfuric acid particles with a mean diameter of about 0.1  $\mu\text{m}$  and concentration from 1 to 10  $\text{cm}^{-3}$  under unperturbed stratospheric conditions. Major volcanic eruptions, such as that of Mt. Pinatubo, may significantly increase the particle size and concentration. Steele and Hamill [1981] first estimated the sulfate aerosol compositions as a function of temperature, predicting aerosol compositions of 70-80 wt % at mid-latitudes and of less than 50 wt % at high latitudes. The global distribution and seasonal variation of the acidity of stratospheric aerosols have been recently compiled by Yue et al. [1994], on the basis of temperature and water partial pressure data obtained by the Stratospheric Aerosol and Gas Experiment 11 (SAGE 11),

1 however, the detailed composition and phase of stratospheric sulfate aerosols have not been firmly established. Present knowledge of phase properties and composition of these aerosols is only inferred indirectly from field observations [Dye et al., 1992; Pueschele et al., 1992; Browell et al., 1993; Rosen et al., 1993; Rinsland et al., 1994]. Also, theoretical predictions of freezing points of sulfate aerosols at stratospheric conditions are severely limited by the lack of fundamental physical parameters concerning surface energies of various sulfuric acid hydrates [Jensen et al., 1991; Luo et al., 1993]. Recently, a number of studies have investigated freezing points of liquid sulfuric acid using bulk solutions [Middlebrook et al., 1993; Ohtake, 1993; Zhang et al., 1993; Beyer et al., 1994; Song, 1994]: many of the studies dealt with rather dilute sulfuric acid, in terms of relevance to PSC formation. For example, crystalline sulfuric acid hydrates such as tetrahydrate and hemihexahydrate [Middlebrook et al., 1993; Zhang et al., 1993] have been proposed to form and persist in certain stratospheric regions.

Both the phase and composition of sulfate aerosols are likely to affect their ability to promote heterogeneous reactions. In the laboratory, the reaction probabilities of reactions 1 to 3 on liquid sulfuric acid have been shown to depend strongly on the acid content: they proceed efficiently in dilute sulfuric acid solutions at low temperatures [Molina et al., 1993; Hanson and Ravishankara, 1994; Zhang et al., 1994a]. Hence, these reactions occurring on stratospheric sulfate aerosols at high latitudes in winter and early spring could provide important pathways for chlorine activation. Outside of the polar regions, the most significant heterogeneous reaction on the sulfate aerosols is believed to be the hydrolysis of  $\text{N}_2\text{O}_5$  (reaction 4) with the consequent changes in the abundance of various nitrogen and chlorine species. Hanson and Ravishankara

[1993] have recently determined that the reaction probability for  $\text{N}_2\text{O}_5$  hydrolysis on crystalline sulfuric acid tetrahydrate (SAT, or a composition of 57.6 wt%) is quite different from that on the liquid surfaces,

Apparently, in addition to studying chemical reactivity of various sulfuric acid hydrates, laboratory investigation of conditions necessary to cause freezing of the supercooled sulfuric acid is also needed. Furthermore, experimental determination of the melting behavior of various sulfuric acid hydrates is important to predicting their stability regions in the stratosphere.

In this work, we investigate sulfuric acid films that simulate stratospheric sulfate aerosols, using a flow tube coupled to a mass spectrometer. We describe freezing point observations of liquid sulfuric acid films at the stratospheric temperatures (190-240 K) and water partial pressures ( $1-4 \times 10^{-4}$  Torr), focusing on concentrated sulfuric acid solutions and possible formation of sulfuric acid monohydrate (SAM, or a composition of 84.5 wt O/O). We also report results of experiments designed to examine melting of SAM films under stratospheric conditions. In addition, BET analysis of gas-adsorption isotherms is performed to characterize the surface roughness and porosities of both SAM and SAT substrates. Finally, reaction probabilities involving  $\text{N}_2\text{O}_5$  and  $\text{ClONO}_2$  with  $\text{H}_2\text{O}$  and  $\text{HCl}$  on SAM films are measured and implications for the stratosphere are discussed.

## Experimental Section

Measurements of freezing/melting points and reaction probabilities were performed in a horizontally mounted flow reactor (2.8-cm i.d.) in conjunction with a mass spectrometer. The detection scheme utilized both electron impact (EI-MS) and chemical ionization (CIMS) mass spectrometry. The majority of the data was taken using EI-MS; the experimental apparatus and procedures were nearly identical to those described by us in a separate publication [Zhang et al., 1994a]. The detailed description about the CIMS apparatus has been given by Leu et al. [1994]. Briefly, the CIMS consisted of an ion flow tube through which a large flow of helium at a pressure of about 0.2 Torr was maintained and where the ion-molecule reactions occurred. The reactant ions,  $\text{H}^+$  or  $\text{SF}_6^+$ , were produced in the ion flow tube by electron attachment to  $\text{CF}_3\text{I}$  or  $\text{SF}_6$ .  $\text{H}^+$  ions were used to selectively detect  $\text{N}_2\text{O}_5$  and  $\text{ClONO}_2$  in the presence of  $\text{HNO}_3$  since  $\text{H}^+$

reacts readily with  $\text{N}_2\text{O}_5$  and  $\text{ClONO}_2$  to produce  $\text{NO}_3^-$  (62 amu) but not with  $\text{HNO}_3$ . At very high  $\text{HNO}_3$  concentrations ( $>10^{11}$  molecules  $\text{cm}^{-3}$ ), some production of  $\text{NO}_3^-$  was also detected due to  $\text{I}^- + \text{HNO}_3$  reaction with  $\text{I}^-$ . By using the relative concentrations of  $\text{I}^-$  and  $\text{HNO}_3$  along with the characteristic reaction time in our system, we estimated a rate coefficient consistent with that suggested by Fehsenfeld et al. [1975].  $\text{SI}_6^-$  reacts with  $\text{N}_2\text{O}_5$ ,  $\text{ClONO}_2$ , and  $\text{HNO}_3$ , yielding  $\text{NO}_3^-$ ,  $\text{I}^- + \text{ClONO}_2$  (116 amu), and  $\text{NO}_3^- + \text{HI}$  (82 amu). Detection sensitivities for these species were approximately  $10^7$ - $10^8$  molecules  $\text{cm}^{-3}$  in the neutral flow tube. Depending on the experimental needs, one of the reactant ions,  $\text{I}^-$  or  $\text{SI}_6^-$ , was employed.

The flow tube was surrounded by an inner jacket in which refrigerated methanol was circulated. The outer jacket of the flow tubes was evacuated to provide thermal insulation. Three movable injectors were located at the upstream end of the flow tube. A heated injector (1.0-cm o.d.) was used to add  $\text{H}_2\text{O}$  (this injector was normally positioned near the upstream end to prevent possible warming of the substrate). The reactants (such as  $\text{ClONO}_2$  or  $\text{N}_2\text{O}_5$ ) were introduced through a centrally-located unjacketed injector (0.3-cm o.d.), and a third injector of similar o.d. was used to introduce other trace species such as  $\text{I}^-$  or  $\text{Cl}^-$ . All the gaseous species were delivered to the flow tube along with small He flows (0.1-5.0  $\text{cm}^3 \text{min}^{-1}$  at S-1) and further diluted in the main He flow (280  $\text{cm}^3 \text{min}^{-1}$  at S-1) before contacting the sulfuric acid surface. Typically, the flow tube was operated at a total pressure of 0.5 Torr and about 890  $\text{cm s}^{-1}$  flow velocity.

Liquid  $\text{H}_2\text{SO}_4$  films were prepared by totally covering the inside walls of the flow tube with sulfuric acid solutions. The thickness of the films was estimated to be about  $\sim 0.1$  mm. To determine the  $\text{H}_2\text{SO}_4$  content of the liquid films, we used the temperature and  $\text{H}_2\text{O}$  partial pressure to convert the  $\text{H}_2\text{SO}_4$  wt %, according to the vapor pressure data of Zeleznik [1991] and Zhang et al. [1993]. The error limit in estimating the  $\text{H}_2\text{SO}_4$  content of the films was about 1-2 wt %, considering uncertainties associated with the temperature and water vapor pressure. Crystallization of the liquid coating can be distinguished visually due to its opaqueness and well-defined crystal structures, as opposite to the liquid state indicated by the clearness and transparency. A photography of the crystalline SAM film formed in the flow tube is shown in Figure 1. Rough surfaces and grain boundaries are clearly evident in this figure, suggesting SAM surface areas should be in general greater than the geometric area of the flow reactor, to be

discussed later. The SAM surfaces were verified to melt within a degree of the pure SAM melting point [Gable et al., 1950]. The temperature and water partial pressure in the flow tube jointly quantified the thermodynamic state of the SAM surfaces [Molina, 1994]: the  $\text{H}_2\text{SO}_4$ -rich and  $\text{H}_2\text{O}$ -rich forms could be generated by controlling the equilibrium  $\text{H}_2\text{O}$  vapor pressure through addition or evaporation of small amounts of water at a constant temperature or by controlling the temperature at a constant  $\text{H}_2\text{O}$  partial pressure,

Reaction probabilities ( $\gamma$ ) were calculated from first-order rate constants ( $k$ ) corresponding to the reactant loss or product growth:

$$\gamma = 2rk/(\omega + k) \quad (6)$$

where  $r$  is the radius of the flow tube and  $\omega$  is the mean thermal velocity of the reactant. To account for the reactant radial and axial gradients in the flow tube which arose when there was a large reactant wall loss, the observed first-order rate constants ( $k_{\text{obs}}$ ) were corrected for gas diffusion by the method suggested by Brown [1978] to obtain  $k$ . The  $\text{ClONO}_2$  and  $\text{N}_2\text{O}_5$  diffusion coefficients in helium used in the Brown calculations were 176 and 171  $\text{cm}^2/\text{s}$  at 200 K and 1 Torr, both with a temperature dependency of  $T^{-1.76}$  [Marrero and Mason, 1972]. These corrections were approximately 10% for small  $\gamma$  values ( $\gamma < 0.01$ ), and as large as a factor of 4 for large  $\gamma$ 's ( $\gamma > 0.2$ ).

The experimental approach for studying surface roughness and porosities of crystalline SAM and SAT was similar to that previously described by Gregg and Sing [1982] and Keyser and Iru [1993]. Briefly, surface area measurements employed the Brunauer, Emmett, and Teller (BET) method to analyze krypton (Kr) adsorption isotherms obtained at 77.2 K. Liquid sulfuric acid films (57.7 and 84.5 wt% for SAT and SAM, respectively) were prepared at the bottom of a glass adsorption cell with a geometric area of  $45\text{ cm}^2$  and frozen at low temperatures. The adsorption cell was then submerged in liquid nitrogen and the isotherms were determined volumetrically by expanding Kr from a calibrated volume at room temperature.

## Results and Discussion

### *Freezing Point Measurements*

We have investigated the supercooling behavior and freezing points of sulfuric acid films using the flowtube/mass spectrometer apparatus. The measurements were carried out by slowly cooling a liquid sulfuric acid film (with an initial  $\text{H}_2\text{SO}_4$  content between 60 and 85 wt%) at less than  $0.1 \text{ K s}^{-1}$ . Upon exhibiting some crystallization, the sample was then held at the constant temperature until completely frozen. A key aspect of the experiment was the maintenance of a constant water partial pressure during freezing. Typically, the crystalline growth was initially quite pronounced and slowly propagated throughout the coating,

Figure 2 depicts the observed freezing temperatures along with the  $\text{H}_2\text{SO}_4$  wt % derived from the  $\text{H}_2\text{O}$  partial pressure and temperature in the flow tube. The equilibrium freezing points of sulfuric acid [Gable et al., 1950] are plotted as the solid curves. The smooth dashed curves represent deliquescence of sulfate aerosols at various stratospheric  $\text{H}_2\text{O}$  mixing ratios [Steele and Hamill, 1981]. Also shown in this figure as the dotted line a-b is the extension of liquid/SAM coexistence curve delineating the SAM stability regime. Figure 2 shows that the observed freezing temperatures depend markedly on the  $\text{H}_2\text{SO}_4$  content. For acid contents between 75 and 85 wt %, the films froze at temperatures between 220 and 250 K; a freezing point maximum occurred for about 85 wt %  $\text{H}_2\text{SO}_4$ . In contrast, dilute sulfuric acid supercooled readily. The films with acid contents between 60 and 75 wt %, as labeled by the horizontal bar, did not freeze, even after being held at 190 K for hours.

In nearly all experiments, we observed that, if the sulfuric acid films froze at temperature and water partial pressures commonly found in the mid- and low latitude stratosphere, SAM was the predominant hydrate. The identity of the frozen substrates was unambiguously confirmed by examining the melting points of the substrates, which matched the literature value of SAM melting point within a degree [Gable et al., 1950]. It is also important to note that the freezing process in our experiments should resemble that occurring in the stratosphere. Additionally, because equilibrium between the condensed and gas phases is actively maintained for sulfate aerosols in the stratosphere, a partially frozen mixture is implausible. If a portion of an 80 wt % acid aerosol droplet freezes to form SAM, for example, the remaining liquid would become more dilute. Subsequently, some of the water in the droplet would evaporate to maintain the constant water partial pressure, but the solid part will continuously grow in such a manner until crystallization is complete.



The extensive supercooling for 60-75 wt %  $\text{H}_2\text{SO}_4$  is consistent with that reported previously [Middlebrook et al., 1993; Ohtake, 1993; Zhang et al., 1993; Beyer et al., 1994; Song, 1994]. Freezing points of more concentrated sulfuric acid ( $> 75$  wt %) have been investigated by Ohtake [1992] and Song [1994] using bulk solutions. While our results are qualitatively similar to those by Song [1994], who also observed a freezing point maximum around the pure SAM composition, this latter study yielded freezing temperatures about 20-30 K lower than the present values for  $\text{H}_2\text{SO}_4$  contents between 75 and 85 wt %. The work of Ohtake [1992] apparently missed this freezing point maximum, presumably due to sparse data collected in this composition range. Both these studies investigated  $\text{H}_2\text{SO}_4$  supercooling in capped test tubes, which may represent non-equilibrium processes. In fact, SAM growth from a solution less than 84.5 wt % could be hindered in a closed system, even if nucleation has been initiated. This occurs because partial freezing of the solution causes a shift in the acid content of the remaining liquid, leading to a more dilute solution. As a result, further growth of SAM can be inhibited, when evaporation of excess  $\text{H}_2\text{O}$  is not possible. An analogue phenomenon has been identified by Middlebrook et al. [1993] involving the freezing of SAT, indicating that addition of water during cooling a  $\text{H}_2\text{SO}_4$  film more concentrated than 57.6 wt % promoted SAT formation.

Note that, although the present supercooling experiments suggest the probable freezing behavior of stratospheric aerosols, they do not provide definitely quantitative information. This is a consequence of the stochastic nature of the nucleation process. Indeed, the crystallization observed in our experiments may be due to heterogeneous nucleation on the glass surfaces. Hence, these observations yield only upper limits to the probable freezing temperatures, since the effects of glass surfaces and large sample sizes in our experiments increase the nucleation rate.

### *Melting of SAM*

While the situation with respect to supercooling and freezing of sulfuric acid films may not be definitive, the melting of SAM can be reasonably defined. This is a process for which the equivalent of supercooling does not take place and hence its occurrence can be predicted reliably using laboratory results or based on thermodynamic considerations.

The melting measurements were performed by first establishing a SAM film in the flow

tube. The substrate temperature was then slowly lowered while keeping a constant water partial pressure. Figure 3 displays a  $P_{\text{H}_2\text{O}}$  versus  $1/T$  phase diagram for the  $\text{H}_2\text{SO}_4/\text{H}_2\text{O}$  binary system. The experimental melting points obtained at different  $\text{H}_2\text{O}$  partial pressures are plotted as open circles. The stability regimes of various sulfuric acid hydrates are also indicated. The shaded area refers to the temperature and  $\text{H}_2\text{O}$  partial pressure conditions likely to be found in the stratosphere. It is evident in this figure that the melting point of the monohydrate depends primarily on the water partial pressure. Essentially, a cooling process at a constant  $\text{H}_2\text{O}$  partial pressure involves transformation of  $\text{H}_2\text{O}$ -rich to  $\text{H}_2\text{SO}_4$ -rich hydrates, accompanied by only a minor change in the bulk composition of the film. This was accomplished by admitting a small amount of  $\text{H}_2\text{O}$  into the system during cooling. The results show that the monohydrate melted upon cooling, that is, when the equilibrium composition was outside the SAM stability region. This implies the absence of a solid-solid phase transformation, i.e., the monohydrate did not transform into any of higher hydrates, but instead it melted at the temperature at which it was in equilibrium with a liquid solution having the same  $\text{H}_2\text{O}$  partial pressure. Nucleation of both di- and tri-hydrates of sulfuric acid has been known to be inefficient [Gable et al., 1950]. These observations are similar to the melting of SAT described previously by Middlebrook et al. [1993] and Zhang et al. [1993] and are consistent with thermodynamic considerations of phase equilibria of the binary system [Wooldridge et al., 1994].

### *Heterogeneous Reactions*

Reaction probabilities on SAM films were obtained from measurements of pseudo-first-order rate coefficients corresponding to the reactant loss. As a first approximation, the surface area of sulfuric acid films was assumed to be the geometric area of the flow tube; potential effects of surface roughness and porosities on the uptake coefficients will be addressed in the next section. The reaction probabilities were studied as a function of thermodynamic state of the substrate, which was adjusted by varying the temperature at a constant  $P_{\text{H}_2\text{O}}$  or by varying  $P_{\text{H}_2\text{O}}$  at a constant temperature.

*$\text{N}_2\text{O}_5$  Hydrolysis.* Figure 4 illustrates typical behavior of the  $\text{N}_2\text{O}_5$  signal as a function of injector position on SAM. The experiment was performed at 210 K and at  $P_{\text{H}_2\text{O}} = 1 \times 10^{-4}$  Torr, equivalent

to a SAM surface of the  $\text{H}_2\text{O}$ -rich form. A  $\text{N}_2\text{O}_5$  partial pressure of about  $4 \times 10^{-7}$  Torr was used in the experiment. It is evident that the lost rate of  $\text{N}_2\text{O}_5$  follows pseudo-first-order kinetics, with a reaction probability of 0.0026 calculated from the rate coefficient. Also shown in this figure for comparison is an experiment performed on a 70 wt% liquid sulfuric acid, yielding a reaction probability of 0.11. On liquid sulfuric acid, this reaction has been shown to be independent of the acid content [e.g., DeMore et al., 1992; Kolb et al., 1994]. The most distinctive feature in this figure is that even on the  $\text{H}_2\text{O}$ -rich SAM the observed uptake coefficient of  $\text{N}_2\text{O}_5$  is about 50-fold slower than that found on liquid acid. This lower reactivity of frozen sulfuric acid may be explained by the nature of the reaction mechanism, which has been suggested to involve dissociation of  $\text{N}_2\text{O}_5$  into  $\text{NO}_3^-$  and  $\text{NO}_2^+$  ions [Mozurkewich and Calvert, 1988]: the occurrence of this dissociation may be suppressed upon freezing.

Figure 5 shows results of the uptake coefficients of  $\text{N}_2\text{O}_5$  on SAM as a function of the  $\text{H}_2\text{O}$  partial pressure at 210 K. In these experiments, the  $\text{N}_2\text{O}_5$  partial pressure was maintained in the range of  $(4-7) \times 10^{-7}$  Torr. The open and filled symbols denote the  $\gamma$ 's measured using FIMS and CI MS, respectively. In general, the differences using these two detection schemes were negligible within the experimental uncertainty, although the uptake appeared to saturate rapidly using FIMS, owing to interference from  $1\text{ HNO}_3$  (both  $\text{N}_2\text{O}_5$  and  $\text{HNO}_3$  were detected at  $m/e = 46$  corresponding to the  $\text{NO}_2^+$  fragment ion in the FIMS). In the isothermal experiments, a readjustment of the  $\text{H}_2\text{O}$  partial pressure in the flow tube was followed by a corresponding change in the thermodynamic state (or in the composition) of the SAM film, occurring mostly on its surface layer [Molina, 1994]. Also, precautions were taken to avoid partial melting of the substrate, which could cause a greater uptake coefficient due to the presence of a small amount of liquid. It is clear in Figure 5 that the uptake coefficient of  $\text{N}_2\text{O}_5$  on SAM exhibits a strong dependence on  $P_{\text{H}_2\text{O}}$ : the value on the  $\text{H}_2\text{O}$ -rich form is about  $10^{-3}$ , whereas it decreases by about an order of magnitude for the acid-rich form. This appears to reflect the reduced chemical potential of  $\text{H}_2\text{O}$  in  $\text{H}_2\text{SO}_4$ -rich surfaces: the tight  $\text{H}_2\text{O}$  bonding in the  $\text{H}_2\text{SO}_4$ -rich surfaces results in a lesser efficiency for  $\text{N}_2\text{O}_5$  to be hydrolyzed. A similar behavior has also been observed for the hydrolysis of  $\text{ClONO}_2$  on nitric acid trihydrate [Abbatt and Molina, 1992] and on sulfuric acid tetrahydrate [Zhang et al., 1994b]. Additional results of the  $\text{N}_2\text{O}_5$  uptake coefficients on SAM are presented in Table I.

Temperature dependence of the uptake coefficients was evaluated by keeping a constant  $\text{H}_2\text{O}$  partial pressure and varying the temperature of the solid, a process also involving transformation of  $\text{H}_2\text{O}$ -rich to  $\text{H}_2\text{SO}_4$ -rich hydrates as the substrate was heated from 190 to 225 K at a  $\text{H}_2\text{O}$  partial pressure ( $\sim 2 \times 10^{-5}$  Torr) in these experiments. These results are given in Figure 6, which plots  $\gamma$  as a function of temperature conducted at  $P_{\text{N}_2\text{O}_5} \sim (4-7) \times 10^{-7}$  Torr. As shown in this figure, there is a marked dependence of  $\gamma$  on temperature: at higher temperature ( $T > 220$  K) the reaction probability was about  $10^{-4}$ , whereas the value approached 0.001 at temperatures near 200 K. Note that the  $\text{H}_2\text{O}$  partial pressure in these experiments was substantially smaller than that normally found in the stratosphere. This is because SAM would melt at much higher temperatures if higher  $P_{\text{H}_2\text{O}}$  were applied, as discussed above.

The  $\text{N}_2\text{O}_5$  hydrolysis on solid SAT substrates has been previously studied by Hanson and Ravishankara [1993]. Our results on  $\text{H}_2\text{O}$ -rich SAM are in general comparable with the reported values by these authors, but their measured  $\gamma$ 's on SAT exhibited little variation with the thermodynamic state of the substrate (or relative humidity in their case).

*$\text{ClONO}_2$  Hydrolysis.* Reaction probability measurements for the  $\text{ClONO}_2$  hydrolysis were conducted in the same manner as those for the  $\text{N}_2\text{O}_5$  hydrolysis. Figure 7 presents the  $\text{ClONO}_2$  signal as a function of injector distance for a SAM substrate at 210 K and a  $\text{H}_2\text{O}$  partial pressure of  $1 \times 10^{-4}$  Torr. The reaction probability for this experiment corresponded to a value of  $\sim 2 \times 10^{-4}$ . Loss of  $\text{ClONO}_2$  on SAM solid was in general very slow, even on the  $\text{H}_2\text{O}$ -rich form. Hence, this value is likely to be interpreted as the upper limit for this reaction on SAM, in addition, such a reaction probability would be consistent with that determined on  $\text{H}_2\text{SO}_4$ -rich SAT [Hanson and Ravishankara, 1993; Zhang et al., 1994b]. An experiment performed on a 65 wt % liquid is also shown in the figure for comparison,  $\text{ClONO}_2$  hydrolysis on liquid sulfuric acid has been shown to depend on the acidic content [e.g., DeMore et al., 1992; Kolb et al., 1994; Zhang et al., 1994a].

*$\text{ClONO}_2$  and  $\text{N}_2\text{O}_5$  Reactions with  $\text{HCl}$ .* The reactive uptakes of  $\text{ClONO}_2$  and  $\text{N}_2\text{O}_5$  by SAM in the presence of  $\text{HCl}$  vapor were studied by first exposing the substrate with  $\text{HCl}$  vapor at the  $\text{HCl}$  partial pressure range of  $(2-8) \times 10^{-7}$  Torr. With  $P_{\text{ClONO}_2}$  and  $P_{\text{N}_2\text{O}_5}$  in the range of  $(2-8) \times 10^{-7}$  Torr and temperatures between 200 and 220 K, there was no observable enhancement in the uptake coefficients over the corresponding hydrolysis values, nor any  $\text{Cl}_2$  or  $\text{ClNO}_2$  production. A

conservative upper limit of  $10^{-4}$  can be placed on both reactions. The very low uptake coefficients of these two reactions on SAH4 are perhaps not surprising, in light of lesser availability of HCl on the SAM surfaces, which has been realized to depend on the water activity [Molina et al., 1993].

### *BET Surface Area Measurements*

A current outstanding issue of heterogeneous chemistry on solid substrates concerns surface roughness and porosities in laboratory simulations of PSCs. The work by Keyser et al. [1991] and Keyser and Irujo [1993] has demonstrated that ice and  $\text{HNO}_3\text{-H}_2\text{O}$  ice films prepared by vapor deposition can be porous, thus affecting reaction probability measurements. This effect is most pronounced for small  $\gamma$ 's where internal diffusion in a porous solid leads to a high number of collisions with the surface. Here we report the first determination of surface areas and porosities of frozen sulfuric acid hydrates. BET surface areas were measured on SAM and SAT films formed in a manner similar to that used to produce the substrates for the flow tube experiments.

A typical Kr adsorption isotherm on crystalline SAM is shown in Figure 8 as a function of relative pressure,  $P/P_0$ , where  $P_0$  is the saturation vapor pressure of the adsorptive. Figure 8 shows that the isotherm is continuous without sharp changes below the saturation pressure; the shape is approximately classified as type II, which is often characterized as monolayer adsorption at low pressures followed by additional multi-layer adsorption with increasing pressures. The amount of Kr adsorbed is related to the surface area of the solid by the BET equation [e.g., Gregg and Sing, 1982],

$$P/[V(P_0 - P)] = 1/(V_m C) + P(C - 1)/(V_m C P_0) \quad (7)$$

where  $V$  is the adsorbed volume in units of  $\text{cm}^3$  at STP,  $V_m$  is the monolayer capacity, and  $C$  is the BET constant. Hence a plot of  $P/[V(P_0 - P)]$  versus the relative pressure should be linear. The BET plot corresponding to the data displayed in Figure 8 is shown in Figure 9. The line through the data is a linear least-squares fit at the relative pressures between 0.05 and 0.4; a surface area of  $0.054 \text{ m}^2 \text{ g}^{-1}$  was inferred from the BET analysis for this particular case. The values for the saturation vapor pressure of Kr at liquid nitrogen temperature and its molecular area used in the

BET analysis were 1.70 Torr and  $20.2 \text{ \AA}^2$ , respectively. Table II summarizes surface area measurements performed on SAM substrates. Several points should be noted in Table II. First, there is no appreciable correlation of the BET area with sample weight under identical experimental conditions. Second, in one experiment, a sample was frozen at about 230 K and then was warmed to higher temperatures for about 30 min. No significant effect of annealing was observed on the surface area. The measured BET surface areas for SAM films were generally greater than the geometric area ( $45 \text{ cm}^2$ ) by a factor of about 5-10, indicating that crystalline SAH4 substrates are moderately porous (which is also consistent with the photography shown in Figure 1). These values, however, are much lower than the BET areas of  $\text{H}_2\text{O}$  and  $\text{HNO}_3\text{-H}_2\text{O}$  ice films formed by vapor deposition [Keyser and Iru, 1993].

For comparison we also performed some experiments on SAT substrates: Figure 10 shows the adsorption isotherm for Kr on a SAT film. This isotherm is qualitatively similar to that for SAM, but the smaller amount of gas adsorbed is indicative of a lower surface area for SAT. The corresponding BET plot is presented in Figure 11. Results of the BET surface area measurements over SAT films are also listed in Table II. As indicated in Table II, the BET surface areas for SAT films are nearly identical to (or only slightly higher than) the geometric area in the adsorption cell, suggesting that the SAT film is likely composed of non-porous crystals. Therefore, the morphology of crystalline SAT appears to be very different from that of crystalline SAM.

For porous solid in general, the interaction of pore diffusion and surface reaction must be considered in order to extract the true reaction probability, as described in detail by Keyser et al. [1991]. The present data reveal that the SAM films formed by freezing liquid sulfuric acid are porous to some extent. Hence, the use of the geometric area, as presented in the preceding section, results in an experimental  $\gamma$  which is an upper limit to the true reaction probability.

### Stratospheric implications

The present results show systematically that concentrated sulfuric acid ( $> 75 \text{ wt } \%$ ) freezes readily to form SAH4 under conditions characteristic of the stratosphere. Furthermore, once formed, SAM can be thermodynamically stable in the temperature range of 22.0-240 K and in the

water partial pressure range of  $(1-4) \times 10^{-4}$  Torr. Note that there are some drawbacks on extrapolating the present freezing observations to the stratosphere because of the stochastic nature of the nucleation process. In the stratosphere, it is likely that the nucleation of SAM may rely on the presence of freezing nuclei.

The melting experiments predict that SAM melts at low temperatures under stratospheric conditions; the stability of SAM is determined by the temperature and water partial pressure. Hence, the regions where SAM may form and persist could be very restricted in the stratosphere. Apparently, warmth and dryness favor the formation of SAM. At a typical stratospheric water mixing ratio of 5 ppmv at 100 mb (corresponding to 16 km), for example, the possibility of SAM existing at temperatures below 220 K can be eliminated. Therefore, if formed, the monohydrate is most likely to be found at mid- and low latitudes, dependent on the temperature and water partial pressure.

The formation of sulfuric acid monohydrate may have important implications for the stratospheric chemistry. Our reaction probability measurements reveal that SAM surfaces are very non-reactive, in particular, the hydrolysis of  $\text{N}_2\text{O}_5$  is significantly suppressed on SAM. This reaction, one of the important heterogeneous reactions occurring on sulfate aerosols, has been known to occur efficiently on liquid sulfate aerosols, with the consequence of affecting the  $\text{NO}_x$  budget and promoting the release of active chlorine. The proposed SAM formation could terminate this reaction channel.

## Conclusions

In this paper we have reported freezing/melting points and heterogeneous chemistry of sulfuric acid monohydrate. By use of a fast flow reactor coupled to mass spectrometric detection, we have investigated sulfuric acid films that simulate stratospheric sulfate aerosols. The results suggest the possible formation of sulfuric acid monohydrate and, consequently, very slow heterogeneous reactions on SAM.

The measurements of BET surface areas show that  $\text{SAH}_4$  films formed by freezing liquid solutions can be porous as are  $\text{H}_2\text{O}$  or  $\text{HNO}_3\text{-H}_2\text{O}$  ice films formed by vapor deposition, albeit to a lesser extent. In contrast, the BET analysis indicates that SAT films are likely composed of

non-porous crystals. This finding justifies earlier laboratory studies in which exterior or geometric surface areas were utilized when deducing reaction probabilities on SAT [Hanson and Ravishankara, 1993; Zhang et al., 1994b].

### **Acknowledgements**

The research described in this paper was performed at the Jet Propulsion Laboratory, California Institute of Technology, under a contract with the National Aeronautics and Space Administration (NASA). We thank M.J. Molina, O. B. T'eeon, and S.C. Wofsy for helpful discussions and C.P. Rinsland for sending preprints of their work.



## References

- Abbatt, J. P. D., and M. J. Molina, Heterogeneous interactions of  $\text{ClONO}_2$  and  $\text{HCl}$  on NAT at 202 K, *J. Phys. Chem.*, 96, 7674-7679, 1992.
- Anderson, J. G., D. W. Toohey, and W. H. Brune, Free radicals within the antarctic vortex: The role of CFCs in antarctic ozone loss, *Science*, 251, 39-46, 1991.
- Beyer, K. D., S. W. Seago, H. Y. Chang, and M. J. Molina, Composition and freezing of aqueous  $\text{H}_2\text{SO}_4/\text{HNO}_3$  solutions under stratospheric conditions, *Geophys. Res. Lett.*, 21, 871-874, 1994.
- Brasseur, G. P., C. Granier, S. Walters, Further changes in stratospheric ozone and the role of heterogeneous chemistry, *Nature*, 346, 626-629, 1991.
- Brown, R. L., Tubular flow reactors with first-order kinetics, *J. Res. Natl. Bur. Stand. U. S.*, 83, 1-8, 1978.
- Browell, E. V., C. F. Butler, M. A. Fenn, W. B. Grant, S. Ismael, M. Schoeberl, O. B. Toon, M. Loewenstein, J. Podolske, Ozone and aerosol changes observed during the 1991-92 Airborne Arctic Stratospheric Expedition, *Science*, 261, 1155-1158, 1993.
- Brune, W. H., J. G. Anderson, D. W. Toohey, D. W. Fahey, S. R. Kawa, R. L. Jones, D. S. McKenna, L. R. Poole, "The potential for ozone depletion in the arctic polar stratosphere," *Science*, 252, 1260-1266, 1991.
- Crutzen, P. J., and F. Arnold, Nitric acid cloud formation in the cold antarctic stratosphere - A major cause for the springtime 'ozone hole', *Nature*, 324, 651-655, 1986.
- DeMore, W. B., S. P. Sander, D. M. Golden, R. F. Hampson, M. J. Kurylo, C. J. Howard, A. R. Ravishankara, C. E. Kolb, and M. J. Molina, *Chemical Kinetics and Photochemical Data for Use in Stratospheric Modeling, Evaluation No. 10, NASA JPL Publ. 92-20*, 1992.
- Dye, J. E., D. Baumgardner, B. W. Gandrud, S. R. Kawa, K. K. Kelly, M. Loewenstein, G. V. Ferry, K. R. Chen, and H. L. Gary, Particle size distributions in arctic polar stratospheric clouds, growth and freezing of sulfuric acid droplets and implications for cloud formation, *J. Geophys. Res.*, 97, 8015-8034, 1992.
- Fehsenfeld, F. C., C. J. Howard, and A. J. Schmeltekopf, Gas-phase ion chemistry of  $\text{HNO}_3$ , *J. Chem. Phys.*, 63, 2835-2841, 1975.

- Gable, C.M., H. F. Betz, and S. H. Mamn, Phase equilibria of the system sulfur trioxide-water, *J. Am. Chem. Soc.*, 72, 1445-1448, 1950.
- Gregg, S. J., and K. S. W. Sing, *Adsorption, surface area and porosity*, Academic Press, New York, 1982.
- Hanson, D. R., and A. Ravishankara, The reaction  $\text{ClONO}_2 + \text{HCl}$  on NAT, NAD, and frozen sulfuric acid and the hydrolysis of  $\text{N}_2\text{O}_5$  and  $\text{ClONO}_2$  on frozen sulfuric acid, *J. Geophys. Res.*, 98, 22,931-22,936, 1993.
- Hanson, D. R., and A. Ravishankara, Reactive uptake of  $\text{ClONO}_2$  onto sulfuric acid due to reaction with  $\text{HCl}$  and  $\text{H}_2\text{O}$ , *J. Phys. Chem.*, 96, 5728-5735, 1994.
- Iofmann, D. R., and S. Solomon, Ozone destruction through heterogeneous chemistry following the eruption of El Chichon, *J. Geophys. Res.*, 94, 5029-5041, 1989.
- Jensen, E. J., O. B. Toon, and P. Hamill, Homogeneous freezing nucleation of stratospheric solution droplets, *Geophys. Res. Lett.*, 18, 1857-1860, 1991.
- Keyser, L. F., S. B. Moore, and M. T. Leu, Surface reaction and pore diffusion in flow-tube reactors, *J. Phys. Chem.*, 95, 5496-5502, 1991.
- Keyser, L. F., and M. T. Leu, Surface areas and porosities of ices used to simulate stratospheric clouds, *J. Colloid and Interface Sci.*, 155, 137-145, 1993.
- Kolb, C. E., D. R. Worsnop, M. S. Zahniser, P. Davidovits, D. R. Hanson, A. Ravishankara, L. F. Keyser, M. T. Leu, L. R. Williams, M. J. Molina, and M. A. Tolbert, laboratory studies of atmospheric heterogeneous chemistry, in *Current Problems in Atmospheric chemistry*, edited by J. R. Barker, *Adv. Phys. Chem.*, in press, 1994.
- Leu, M. T., R. S. Timonen, L. F. Keyser, and Y. I. Yung, Heterogeneous reactions of  $\text{NO}_2 + \text{NaCl} \rightarrow \text{HCl} + \text{NaNO}_3$  and  $\text{N}_2\text{O}_5 + \text{NaCl} \rightarrow \text{ClONO}_2 + \text{NaNO}_3$ , manuscript in preparation, 1994.
- Luo, B. P., Th. Peter, and P. J. Crutzen, Maximum supercooling of  $\text{H}_2\text{SO}_4$  acid aerosol droplets, *Ber. Bunsen Ges. Phys. Chem.*, 96, 334-338, 1992.
- Marrero, T. R., and E. A. Mason, Gaseous diffusion coefficients, *J. Phys. Chem. Ref. Data*, 1, 3-118, 1972.
- Middlebrook, A. M., L. P. Iraci, L. S. McNeill, B. G. Koehler, M. A. Wilson, O. W. Saastad, M. A. Tolbert, and D. R. Hanson, Fourier transform-infrared studies of thin  $\text{H}_2\text{SO}_4/\text{H}_2\text{O}$

- films: formation, water uptake, and solid-liquid phase changes, *J. Geophys. Res.*, **98**, 20,437-20,481, 1993.
- Molina, M. J., in *CHEMRAW VII: Chemistry of the Atmosphere: The impact of global change*, edited by J. G. Calvert, Oxford University Press, London, 1994.
- Molina, M. J., R. Zhang, P. J. Wooldridge, J. R. McMahon, J. E. Kim, J. Y. Chang, and K. D. Beyer, Physical chemistry of the  $\text{H}_2\text{SO}_4/\text{HNO}_3/\text{H}_2\text{O}$  system: Implications for polar stratospheric clouds, *Science*, **261**, 1418-1423, 1993.
- Mozurkewich, M., and J. G. Calvert, Reaction probability of  $\text{N}_2\text{O}_5$  on aqueous aerosols, *J. Geophys. Res.*, **93**, 5,889-5,896, 1988.
- Ohtake, T. Freezing points of  $\text{H}_2\text{SO}_4$  aqueous solution and formation of stratospheric clouds, *Tellus*, **45B**, 138-144, 1993.
- Pueschel, R. F., G. V. Ferry, K. G. Snetsinger, J. Goodman, J. E. Dye, D. Baumgardner, and B. W. Gandrud, A case of type 1 polar stratospheric cloud formation by heterogeneous nucleation, *J. Geophys. Res.*, **97**, 8105-8114, 1992.
- Rinsland, C. P., G. K. Yue, M. R. Gunson, R. Zander, and M. C. Abrams, Mid-infrared extinction by sulfate aerosols from the Mt. Pinatubo eruption, *J. Quant. Spectrosc. Radiat. Transfer*, submitted, 1994.
- Rodriguez J. M., M. K. W. Ko, and N. D. Sze, Role of heterogeneous conversion of  $\text{N}_2\text{O}_5$  on sulfate aerosols in global ozone losses, *Nature*, **352**, 134-137, 1991.
- Rosen, J. M., N. T. Kjome, and S. J. Oltmans, Simultaneous ozone and polar stratospheric cloud observation at south pole during winter and spring, *J. Geophys. Res.*, **96**, 12,741-12,751, 1993.
- Solomon, S., The mystery of the Antarctic ozone 'hole', *Rev. Geophys.*, **26**, 131-148, 1988.
- Song, N., Freezing temperatures of  $\text{H}_2\text{SO}_4/\text{HNO}_3/\text{H}_2\text{O}$  mixtures: implications for polar stratospheric clouds, *Geophys. Res. Lett.*, submitted, 1994.
- Steele H. M. and P. Hamill, Effects of temperature and humidity on the growth and optical properties of sulfuric acid-water droplets in the stratosphere, *J. Aerosol Sci.*, **12**, 517-528, 1981.
- Seaton, O. B., P. Hamill, R. P. Turco, and J. Pinto, Condensation of  $\text{HNO}_3$  and  $\text{HCl}$  in the winter polar stratosphere, *Geophys. Res. Lett.*, **13**, 1284-1287, 1986.

- Yuc, G. K., L. R. Poole, P. J. Wang, and F. W. Chiou, Stratospheric aerosol acidity, density, and refractive index deduced from SAGE II and NMC temperature data, *J. Geophys. Res.*, **99**, 3727-3738, 1994.
- Webster, C. R., R. D. May, D. W. Toohey, L. M. Avallone, J. G. Anderson, P. Newman, L. Lait, M. R. Schoeberl, J. W. Elkins, K. R. Chan, Chlorine chemistry on polar stratospheric cloud particles in the arctic winter, *Science*, **261**, 1130-1134, 1993.
- Wooldridge, P. J., R. Zhang, and M. J. Molina, Phase equilibria of  $\text{H}_2\text{SO}_4$ ,  $\text{HNO}_3$ , and  $\text{HCl}$  hydrates and the composition of polar stratospheric clouds, *J. Geophys. Res.*, in press, 1994.
- Zelevnik, F. Thermodynamic properties of the aqueous sulfuric acid system to 350 K, *J. Phys. Chem. Ref. Data*, **20**, 1157-1200, 1991.
- Zhang, R., P. J. Wooldridge, J. P. D. Abbatt, and M. J. Molina, Physical chemistry of the  $\text{H}_2\text{SO}_4/\text{H}_2\text{O}$  binary system at low temperatures: Stratospheric implications, *J. Phys. Chem.*, **97**, 7351-7358, 1993.
- Zhang, R., M. T. Leu, and L. F. Kucser, Investigation of heterogeneous reactions of  $\text{ClONO}_2$ ,  $\text{HCl}$ , and  $\text{HOCl}$  on liquid sulfuric acid surfaces, *J. Phys. Chem.*, in press, 1994a.
- Zhang, R., J. P. Jayne, and M. J. Molina, Heterogeneous interactions of  $\text{ClONO}_2$  and  $\text{HCl}$  with sulfuric acid tetrahydrate: implications for the stratosphere, *J. Phys. Chem.*, **96**, 867-874, 1994b.

Table 1. Uptake Coefficients of the 1 hydrolysis of  $\text{N}_2\text{O}_5$  on SAM<sup>a</sup>

$T$ (K)	$P_{\text{H}_2\text{O}}$ (Torr)	$P_{\text{N}_2\text{O}_5}$ (Torr)	
230	$3.6 \times 10^{-4}$	$4.7 \times 10^{-7}$	$7.5 \times 10^{-4}$
230	$2.8 \times 10^{-4}$	$5.2 \times 10^{-7}$	$5.9 \times 10^{-4}$
230	$2.1 \times 10^{-4}$	$6.0 \times 10^{-7}$	$5.2 \times 10^{-4}$
220	$2.1 \times 10^{-4}$	$5.2 \times 10^{-7}$	$9.1 \times 10^{-4}$
220	$1.5 \times 10^{-4}$	$5.3 \times 10^{-7}$	$8.5 \times 10^{-4}$
215	$1.1 \times 10^{-4}$	$5.6 \times 10^{-7}$	$1.1 \times 10^{-3}$

<sup>a</sup> Data obtained using CIMS.

Table 11. BET Surface Areas of crystalline  $\text{H}_2\text{SO}_4$  Hydrates<sup>a</sup>

Substrate	Weight (g)	Monolayer <sup>b</sup> ( $\mu\text{moles g}^{-1}$ )	BET constant	Surface area <sup>b</sup> ( $\text{m}^2 \text{g}^{-1}$ )
SAM	0.592.	<b>0.422</b>	<b>48.8</b>	0.051
SAM	0.40s	<b>0.444</b>	<b>79.3</b>	0.054
SAM	0.596	<b>0.331</b>	<b>64.8</b>	0.040
SAM <sup>c</sup>	0.685	<b>0.306</b>	<b>82.2</b>	0.037
SAM	1.120	<b>0.3s3</b>	<b>58.7</b>	0.043
				av = 0.045 $\pm$ 0.0073 (1 $\sigma$ )
SAT	0.188	0.215	<b>24.6</b>	0.026
SAT	0.324	0.186	<b>22.8</b>	0.023
				av = 0.025 $\pm$ 0.0022 (1 $\sigma$ )

<sup>a</sup> Adsorbate gas was Kr and the crystalline hydrates were made from freezing liquid solutions; geometric area of the sulfuric acid films was 45 cm<sup>2</sup>.

<sup>b</sup> Sulfuric acid surface area was obtained by subtracting the cold Pyrex surface area in the adsorption cell, ~ 145 cm<sup>2</sup>.

<sup>c</sup> Sample was annealed to 273 K for about 30 min after freezing.

## Figure Captions

- Figure 1. A crystalline SAM film formed in the flow tube by freezing liquid solutions at 220 K. See text for details.
- Figure 2. Freezing temperatures of various  $\text{H}_2\text{SO}_4$  solutions studied in the flow tube/mass spectrometer apparatus. Weight percents at the freezing points (open triangle) were calculated from the temperature and  $\text{H}_2\text{O}$  vapor pressure, based on  $\text{H}_2\text{O}$  vapor pressure data of the  $\text{H}_2\text{SO}_4/\text{H}_2\text{O}$  solutions from Zeleznik [1991] and Zhang et al. [1993]. Also shown in this figure is the freezing envelop of sulfuric acid [Gable et al., 1950]. The horizontal bar denotes the composition range over which the films were held at temperatures below 190 K without freezing. The dotted line a-b corresponds to the extension of the coexistence line between liquid and SAM. The smooth dashed curves represent equilibrium sulfuric acid compositions of stratospheric aerosols at  $\text{H}_2\text{O}$  mixing ratios of 5.0, 3.0, and 1.5 ppmv at 100 mb (corresponding to about 16 km).
- Figure 3. Observed melting temperatures (open circles) of sulfuric acid monohydrate (SAM) plotted in a  $P_{\text{H}_2\text{O}}$  versus  $1000/T$  phase diagram [Zeleznik, 1991; Zhang et al., 1993]. The shaded area corresponds to temperature and  $\text{H}_2\text{O}$  partial pressure conditions likely to be found in the mid- and low latitude stratosphere. The dotted line a-b is as in Figure 2. The data show that SAM can be thermodynamically stable in the temperature range of 220-240 K and in the water partial pressure range of  $(1-4) \times 10^{-4}$  Torr and that SAM melts when the temperature and equilibrium  $\text{H}_2\text{O}$  vapor pressure are outside of its stability regime.
- Figure 4.  $\text{N}_2\text{O}_5$  signals as a function of injector position for an experiment performed on a SAM film at 210 K and  $P_{\text{H}_2\text{O}} \approx 1 \times 10^{-4}$  Torr (solid line, solid circles). Also shown for comparison is an experiment on a 70 wt %  $\text{H}_2\text{SO}_4$  liquid film at 218 K (dashed line, open circles). Both experiments were carried out using CIMS. Experimental conditions:  $P_{\text{N}_2\text{O}_5} = 4 \times 10^{-7}$  Torr,  $P_{\text{He}} = 0.4$  Torr, and flow velocity  $\approx 1800$  cm s<sup>-1</sup>.
- Figure 5. Reaction probability of  $\text{N}_2\text{O}_5$  with  $\text{H}_2\text{O}$  as a function of  $P_{\text{H}_2\text{O}}$  on SAM surfaces at 210 K. The open and filled symbols refer to measurements using FIMS and

CIMS, respectively. Experimental conditions:  $P_{\text{N}_2\text{O}_5} = (4-7) \times 10^{-7}$  Torr,  $P_{\text{He}} = 0.4$  to  $0.5$  Torr, flow velocity = 810 to 1800 cm S-1, and  $T = 210$  K,

Figure 6. Reaction probability of  $\text{N}_2\text{O}_5$  with  $\text{H}_2\text{O}$  as a function of temperature on SAM surfaces. The open and filled symbols refer to measurements using FIMS and CIMS, respectively. Experimental conditions:  $P_{\text{N}_2\text{O}_5} = (4-7) \times 10^{-7}$  Torr,  $P_{\text{He}} = 0.4$  to  $0.5$  Torr, velocity = 810 to 1800 cm s<sup>-1</sup>, and  $P_{\text{H}_2\text{O}} = 2 \times 10^{-5}$  Torr.

Figure 7.  $\text{ClONO}_2$  signals as a function of injector position for experiments performed on a SAM film at 210 K and  $P_{\text{H}_2\text{O}} \approx 1 \times 10^{-4}$  Torr (solid line, filled circles) and on a 65 wt % liquid  $\text{H}_2\text{SO}_4$  film at 212 K. Both experiments were carried out using CIMS. Experimental conditions:  $P_{\text{ClONO}_2} \approx 4 \times 10^{-7}$  Torr,  $P_{\text{He}} = 0.4$  Torr, and flow velocity  $\approx 1800$  cm s<sup>-1</sup>.

Figure 8. Adsorption isotherm of Kr on 0.405 g of crystalline SAM (84.5 wt %) at 77.5 K.

Figure 9. BET plot of  $P/V(P_0 - P)$  against  $P/P_0$  for the data displayed in Figure 8.

Figure 10. Adsorption isotherm of Kr on 0.188 g of crystalline SAT (57.6 wt %) at 77.5 K.

Figure 11. Same as Figure 9 except for the data displayed in Figure 10.



14 mm

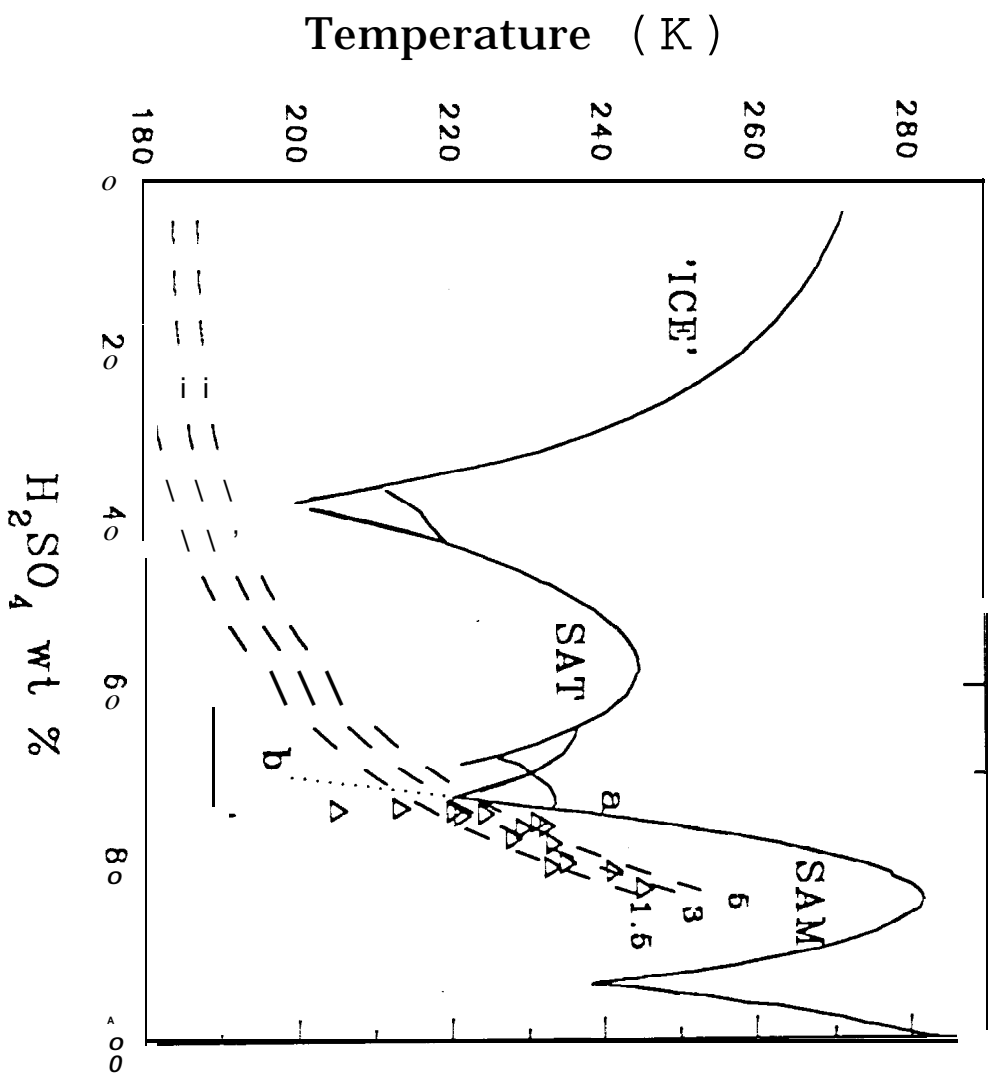


Fig. 2

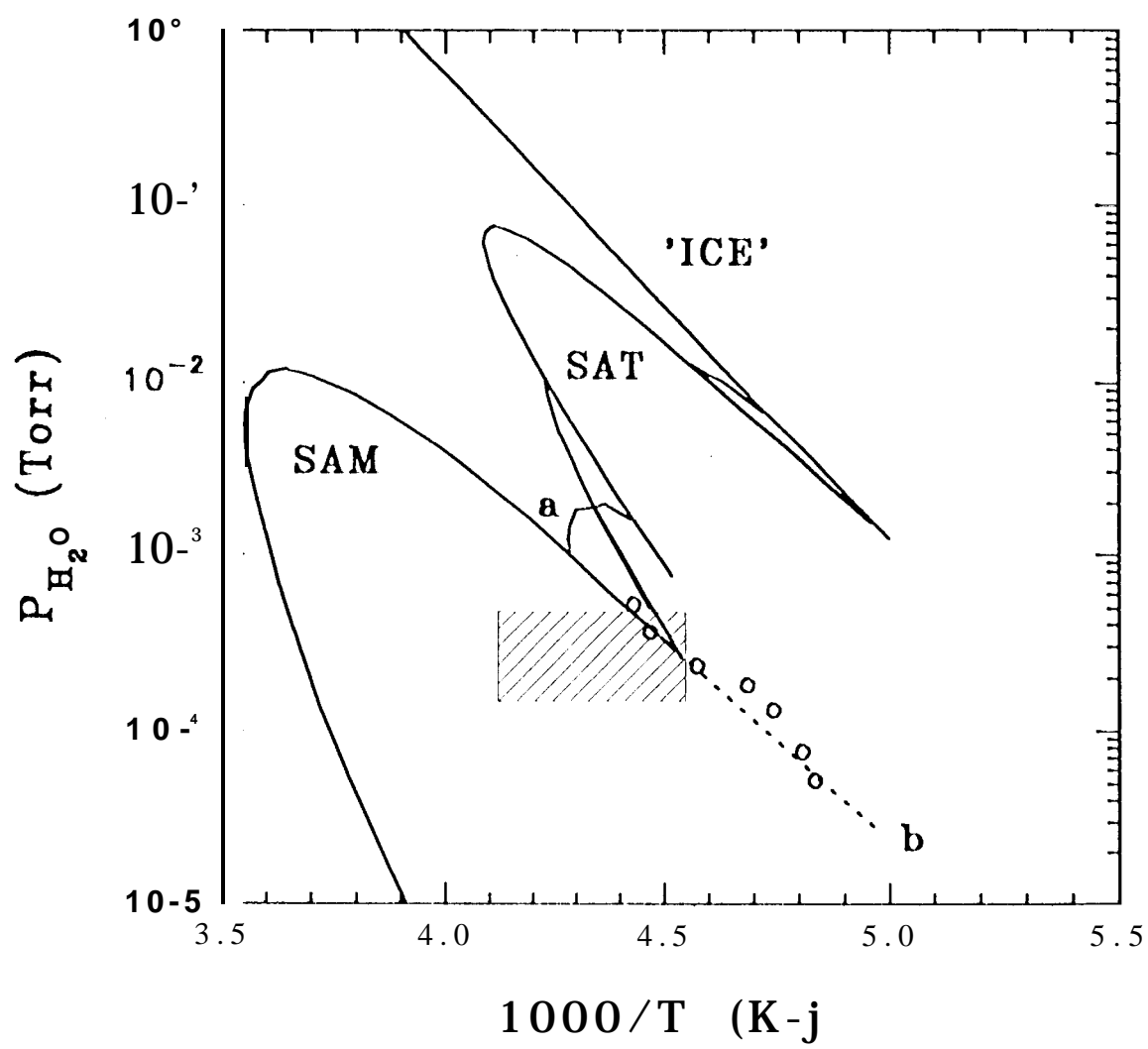


Fig. 3

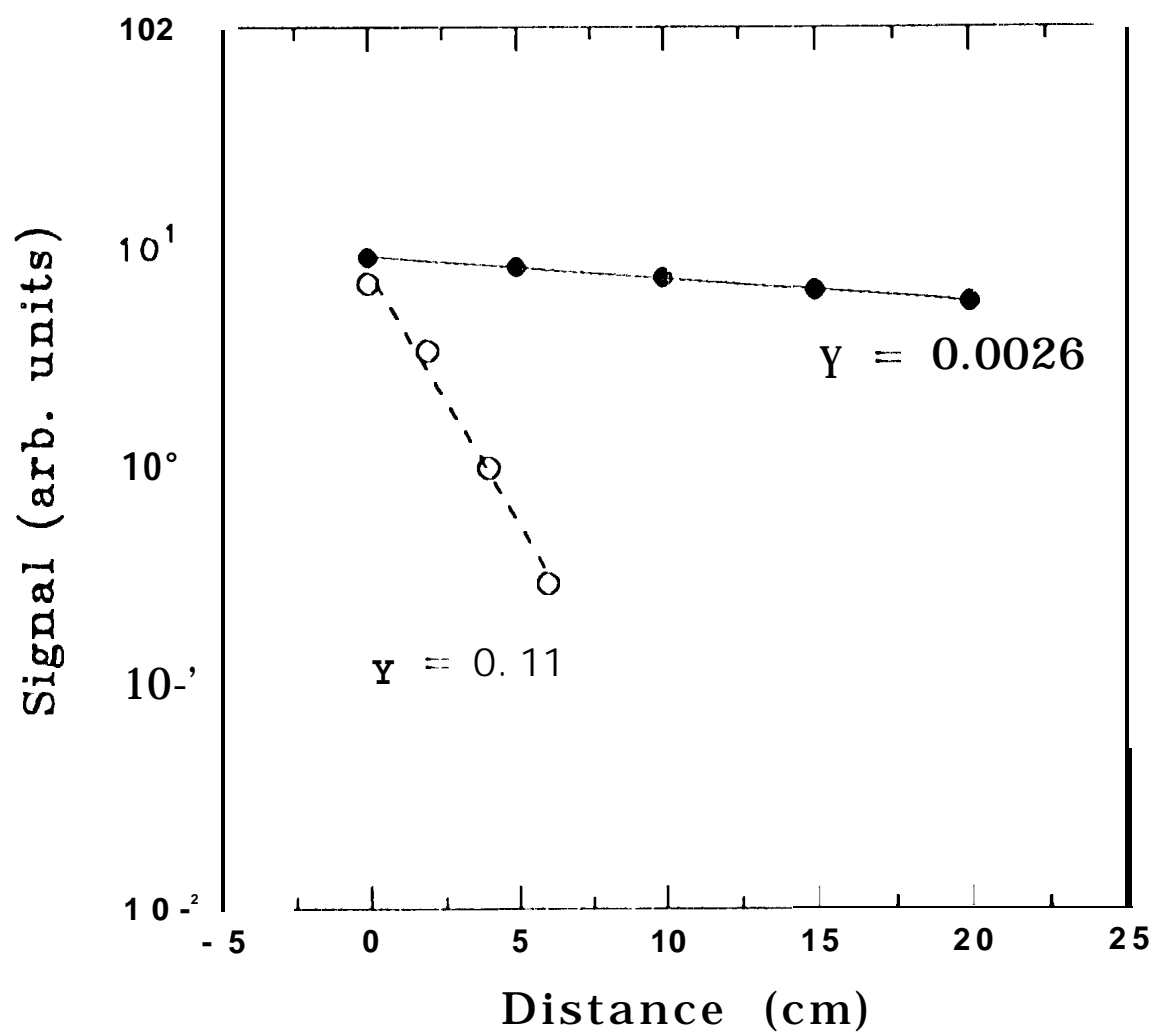


Fig 6

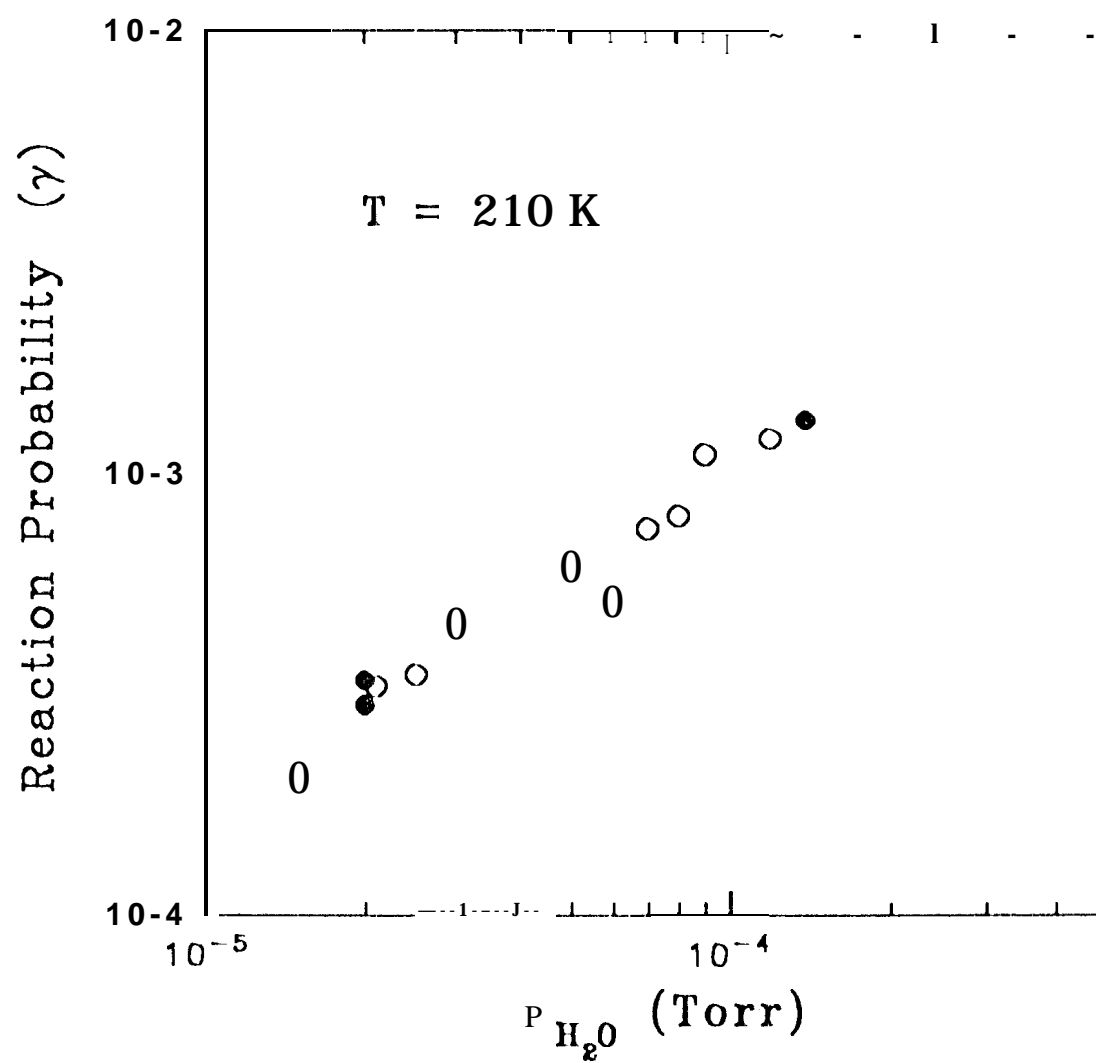


Fig. 5

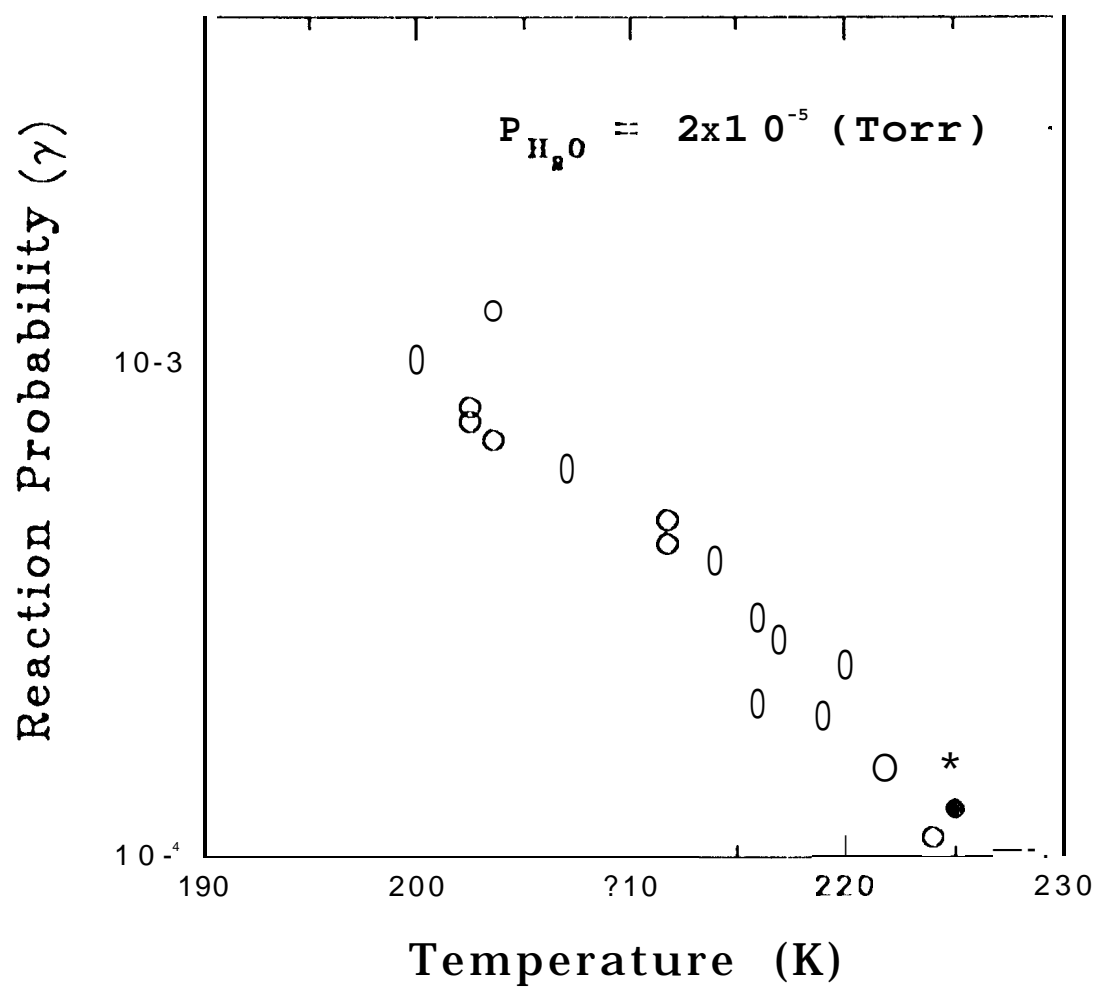
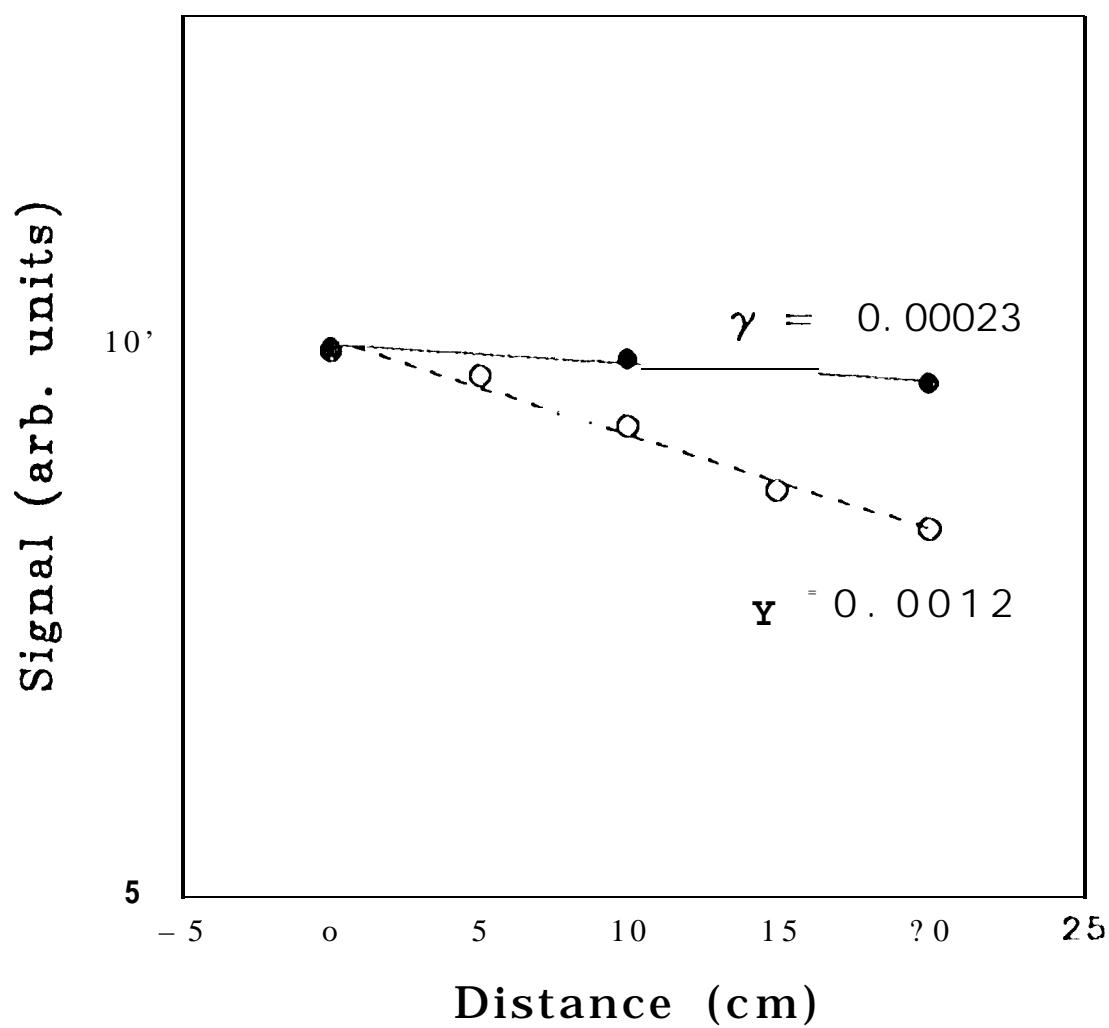
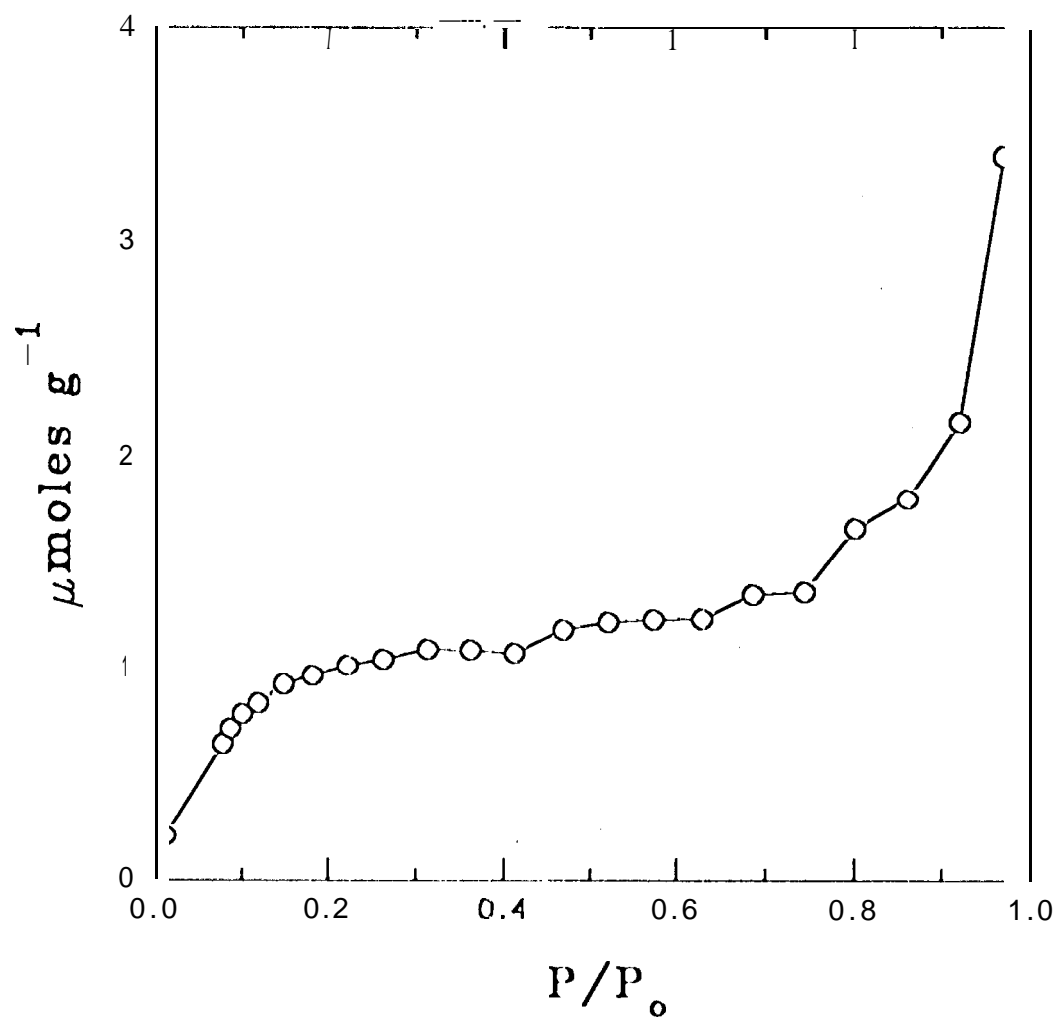


Fig 6



F-27





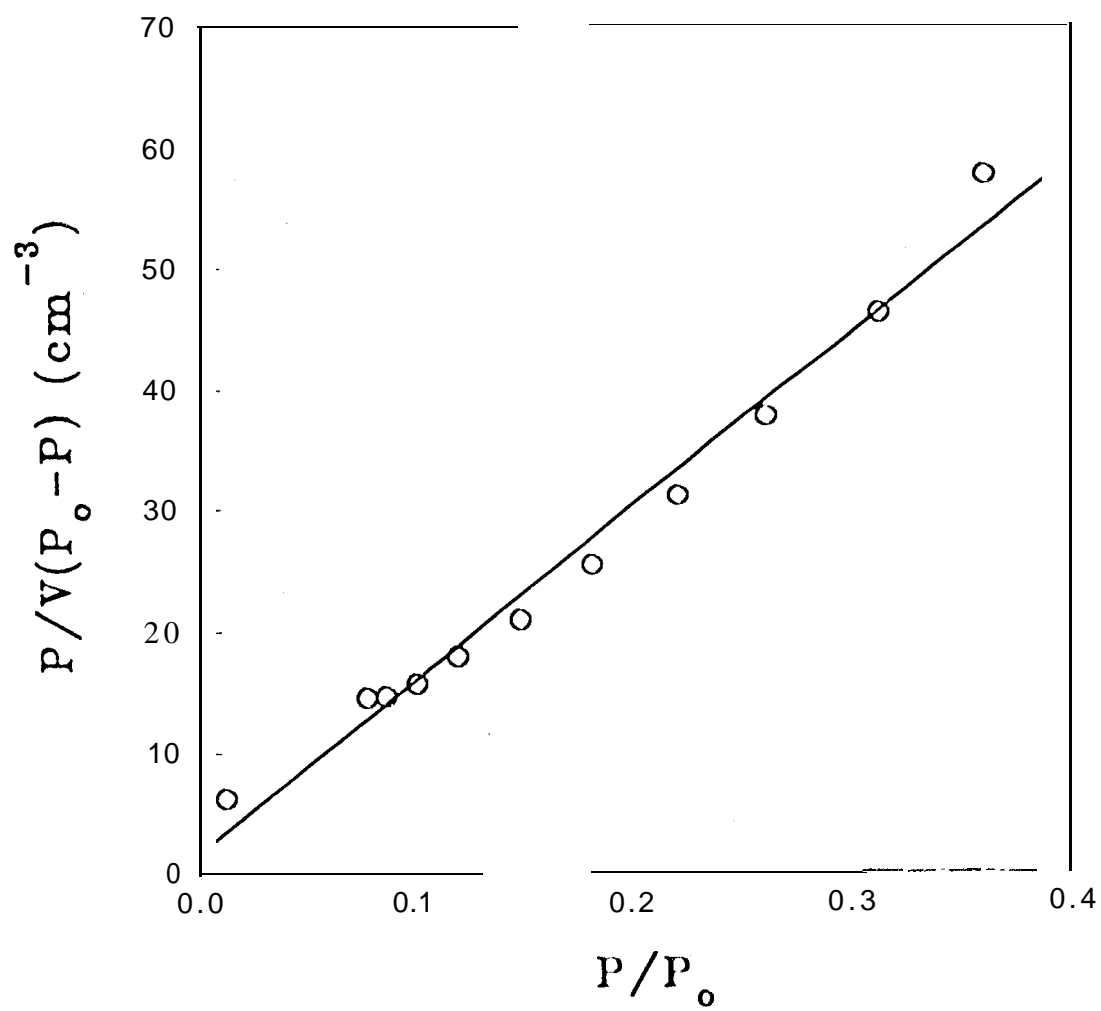


Fig. 9

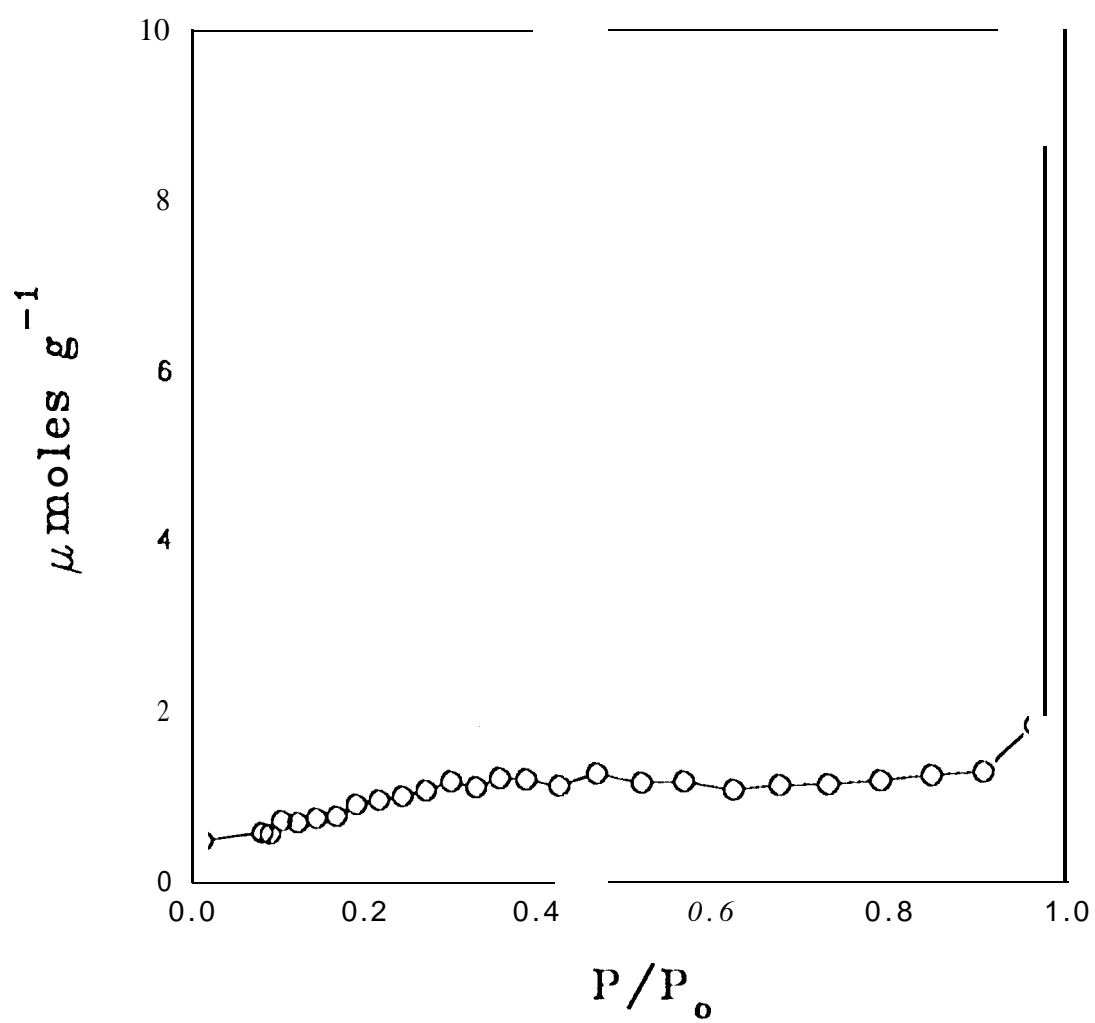


Fig. 10

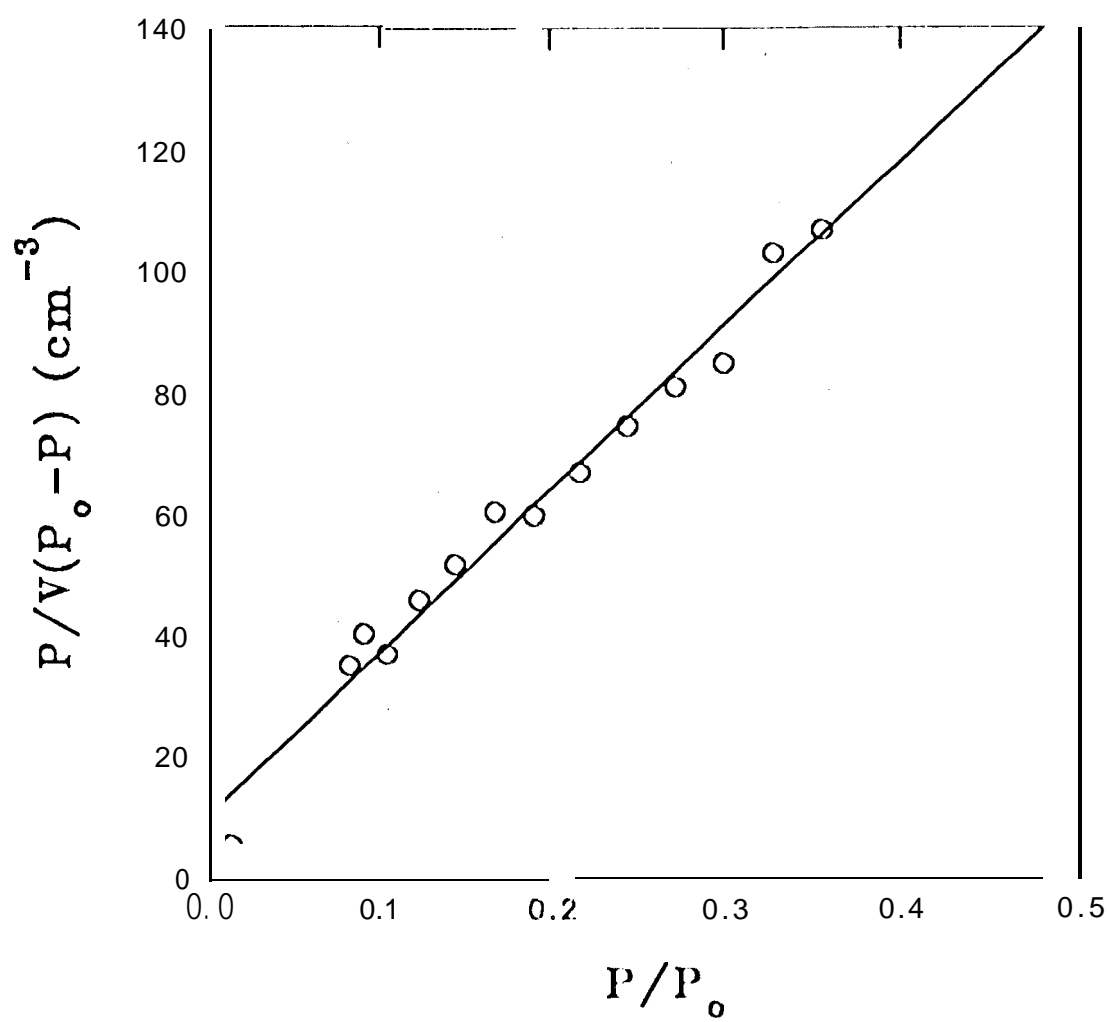


Fig. 10